



Article

# Evaluation of Toxic Amyloid $\beta$ 42 Oligomers in Rat Primary Cerebral Cortex Cells and Human iPS-derived Neurons Treated with 10-Me-Aplog-1, a New PKC Activator

Kazuma Murakami <sup>1,\*</sup>, Mayuko Yoshimura <sup>1</sup>, Shota Nakagawa <sup>2</sup>, Toshiaki Kume <sup>2,3</sup>, Takayuki Kondo <sup>4,5,6</sup>, Haruhisa Inoue <sup>4,5,6</sup> and Kazuhiro Irie <sup>1,\*</sup>

<sup>1</sup> Division of Food Science and Biotechnology, Graduate School of Agriculture, Kyoto University, Kyoto 606-8502, Japan; myk0128dw@gmail.com

<sup>2</sup> Department of Pharmacology, Graduate School of Pharmaceutical Sciences, Kyoto University, Kyoto 606-8501, Japan; nakagawa.shota.0812@gmail.com (S.N.); tkume@pha.u-toyama.ac.jp (T.K.)

<sup>3</sup> Department of Applied Pharmacology, Graduate School of Medicine and Pharmaceutical Sciences, University of Toyama, Toyama 930-0194, Japan

<sup>4</sup> Center for iPS Cell Research and Application (CiRA), Kyoto University, Kyoto 606-8507, Japan; takayuki.kondo@cira.kyoto-u.ac.jp (T.K.); haruhisa@cira.kyoto-u.ac.jp (H.I.)

<sup>5</sup> iPSC-based Drug Discovery and Development Team, RIKEN BioResource Research Center (BRC), Kyoto 619-0237, Japan

<sup>6</sup> Medical-risk Avoidance based on iPS Cells Team, RIKEN Center for Advanced Intelligence Project (AIP), Kyoto 606-8507, Japan

\* Correspondence: alzkazu@kais.kyoto-u.ac.jp (K.M.); irie@kais.kyoto-u.ac.jp (K.I.); Tel.: +81-75-753-6282 (K.M.); +81-75-753-6281 (K.I.)

Received: 15 January 2020; Accepted: 6 February 2020; Published: 11 February 2020



**Abstract:** Amyloid  $\beta$ 42 ( $A\beta$ 42), a causative agent of Alzheimer's disease (AD), is derived extracellularly from  $A\beta$  precursor protein (APP) following the latter's cleavage by  $\beta$ -secretase, but not  $\alpha$ -secretase. Protein kinase C $\alpha$  (PKC $\alpha$ ) activation is known to increase  $\alpha$ -secretase activity, thereby suppressing  $A\beta$  production. Since  $A\beta$ 42 oligomer formation causes potent neurotoxicity, APP modulation by PKC ligands is a promising strategy for AD treatment. Although bryostatin-1 (bryo-1) is a leading compound for this strategy, its limited natural availability and the difficulty of its total synthesis impedes further research. To address this limitation, Irie and colleagues have developed a new PKC activator with few side effects, 10-Me-Aplog-1, (**1**), which decreased  $A\beta$ 42 in the conditioned medium of rat primary cerebral cortex cells. These results are associated with increased  $\alpha$ -secretase but not PKC $\epsilon$ -dependent  $A\beta$ -degrading enzyme. The amount of neuronal embryonic lethal abnormal vision (nELAV), a known  $\beta$ -secretase stabilizer, was reduced by treatment with **1**. Notably, **1** prevented the formation of intracellular toxic oligomers. Furthermore, **1** suppressed toxic oligomerization within human iPS-derived neurons such as bryo-1. Given that **1** was not neurotoxic toward either cell line, these findings suggest that **1** is a potential drug lead for AD therapy.

**Keywords:** alzheimer's disease; amyloid  $\beta$ ; bryostatin-1; ECE1; iPS; nELAV; neurotoxicity; oligomer; protein kinase C;  $\alpha$ -secretase

## 1. Introduction

The 40-mer and 42-mer amyloid  $\beta$ -proteins ( $A\beta$ 40 and  $A\beta$ 42) are considered causative agents of Alzheimer's disease (AD) [1,2].  $A\beta$ 40 and  $A\beta$ 42 are known to be produced from  $A\beta$  precursor protein (APP) following cleavage of the latter by  $\beta$ -secretase, but not  $\alpha$ -secretase. APP proteolysis may

be more complex, given the recent discovery of APP proteolysis by  $\eta$ - and  $\delta$ -secretases, for example, in [3]. The ability of A $\beta$ 42 to aggregate and exhibit neurotoxicity is higher than that of A $\beta$ 40 despite the lower in vivo amounts of A $\beta$ 42 [4]. A $\beta$ 42 oligomer formation causes synaptic dysfunction and neuronal death in AD pathology, whereas the contribution of end-stage mature fibrils of A $\beta$ 42 to AD is lower than that of oligomers [5]. Higher-order toxic oligomers that show potent synaptotoxicity and neurotoxicity have been reported, such as protofibrils (PFs), A $\beta$ -derived diffusible ligands, and amylospheroids [6]. Therefore, suppressing toxic oligomerization of A $\beta$ 42 is a favorable strategy for developing AD therapies. This suppression can also be achieved by simultaneously decreasing A $\beta$  production while inducing A $\beta$  degradation.

Protein kinase C (PKC) is a family of serine/threonine kinases that plays a pivotal role in various biological events such as signal transduction, proliferation, and apoptosis mediated by the second messenger 1,2-diacyl-*sn*-glycerol [7]. The PKC family, which contains at least 10 isozymes, is divided into three groups, namely conventional ( $\alpha$ ,  $\beta$ I,  $\beta$ II, and  $\gamma$ ), novel ( $\delta$ ,  $\epsilon$ ,  $\eta$ , and  $\theta$ ), and atypical ( $\mu$ ,  $\xi$ , and  $\iota$ ) [7]. PKC activity is related to memory formation and learning [8], while PKC downregulation may induce cognitive impairment and memory loss in AD [9]. Regarding A $\beta$ -driven molecular events, PKC $\alpha$  reportedly upregulates  $\alpha$ -secretase activity either directly or indirectly through the mitogen-activated protein kinase (MAPK) pathway [10]. PKC $\alpha$  activation in a mouse model of AD has beneficial effects on AD pathology, including the disruption of A $\beta$  production and reduction of toxic A $\beta$  oligomer formation [11]. Neuronal embryonic lethal abnormal vision (nELAV), also known as HuD protein, may contribute to mRNA stability through a PKC $\alpha$ -dependent mechanism due to adenine- and uridine-rich elements (AREs) [12]. PKC $\epsilon$  may also be a target beneficial for preventing AD. A mouse study demonstrated that PKC $\epsilon$  activation reduces senile plaque formation, although its effect on oligomer generation was not determined [13]. Similarly, the stimulator specific for PKC $\epsilon$  (DCP-LA) rescued synaptic dysfunction and cognitive deficits as well as senile plaques in another mouse study [14]. PKC $\epsilon$  stimulates the degradation of A $\beta$ 42 and A $\beta$ 40 by activating endothelin converting enzyme 1 (ECE1) [15]. These reports indicate that PKC activation may offer a promising strategy for AD treatment.

Bryostatin-1 (bryo-1), which was isolated from the marine bryozoan *Bugula neritina* [16], is a potent PKC activator with few side effects such as tumor-promoting and proinflammatory activities. Bryo-1 was found to activate both PKC $\alpha$  and PKC $\epsilon$ , and to restore loss of hippocampal synapses and memory impairment by suppressing the levels of A $\beta$  oligomers detected by the A11 antibody [14]. Bryo-1 may have beneficial effects against A $\beta$ -induced abnormality in human fibroblasts [17]. These findings indicate that bryo-1 is a potential drug lead for AD [18]. However, its limited availability from natural sources and the difficulty of total synthesis both hamper further development, despite scalable synthetic routes reported by the Wender [19] and Trost groups [20]. Taking an alternative approach, Irie and colleagues developed 10-Me-Aplog-1 (**1**; Figure 1a), a simplified analog of aplysiatoxin [21], which is a potent PKC activator with tumor-promoting activity. It should be noted that **1** exhibited anti-proliferative activity towards cancer cell lines without significant tumor-promoting or proinflammatory activities [22,23].

The ratio of A $\beta$ 42 to A $\beta$ 40 (A $\beta$ 42/A $\beta$ 40) is a known biomarker for predicting AD onset in cerebrospinal fluid (CSF) and plasma [24]. However, such a biomarker could correlate with senile plaque depositions containing less toxic fibrils according to brain imaging of A $\beta$  deposition with positron emission tomography (A $\beta$ -PET) [25–27]. Furthermore, the PKC activation strategy is not expected to modulate A $\beta$ 42/A $\beta$ 40, since the proteolysis of APP by  $\gamma$ -secretase can predominantly determine the length of secreted A $\beta$ .

Irie and colleagues identified a toxic A $\beta$ 42 conformer with a turn at positions 22–23 (toxic turn) [28], and proposed the ratio of the toxic conformer to total A $\beta$ 42 as a possible biomarker for AD progression in CSF using sandwich ELISA specific for A $\beta$ 42 toxic oligomers based on the anti-toxic turn antibody (24B3) [29]. A change in A $\beta$ 42 toxic conformer ratio may be a good predictor for long-term cognitive outcomes in idiopathic normal pressure hydrocephalus (iNPH) [30]. Toxic conformers can easily form

toxic oligomers [31]. Here, we offer a novel, direct evaluation platform that determines the ratio of toxic oligomers to A $\beta$ 42 (toxic oligomers/A $\beta$ 42) in rat primary cerebral cortex cells and human induced pluripotent stem (iPS)-derived neurons using 24B3-based ELISA [29], which were treated with **1**. The therapeutic potential of **1** and its mechanism of action in AD prevention were also investigated.

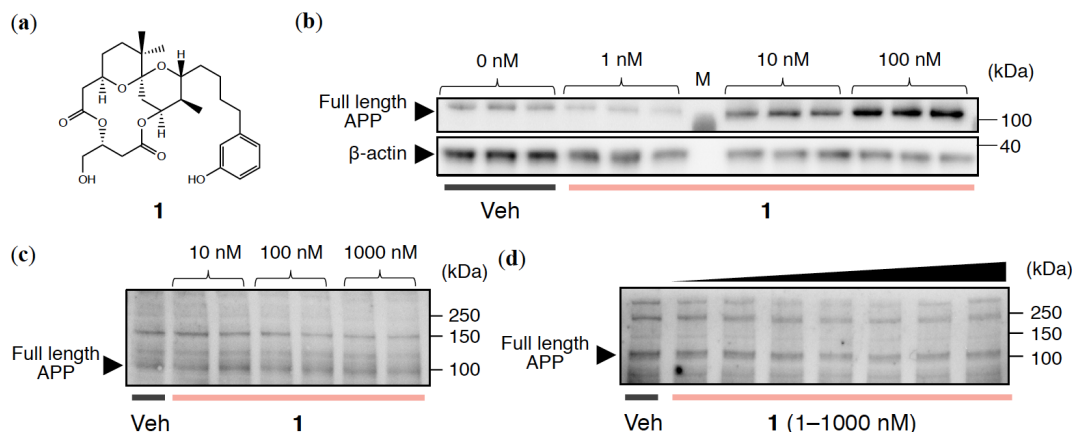


**Figure 1.** (a) Structure of 10-Me-Aplog-1 (**1**). APP expression levels in (b) HEK293-APPwt, (c) SH-SY5Y, and (d) rat primary cerebral cortex cells treated with **1** at the indicated concentrations for 24 h. M indicates marker. In (d), 1, 10, 50, 100, 500, and 1000 nM (from left to right) of **1** were used. Veh: vehicle.

## 2. Results

### 2.1. APP Expression Levels in Cultured Neuronal Cell Lines Treated with **1**

The reason why research on PKC modulators faces difficulties in the AD field is the abnormal enhancement of APP itself upon addition of PKC ligand to cultured animal cells, including rat PC12 cells [32] and human HeLa cells [33], resulting in unwanted A $\beta$  overproduction. Alternatively, APP secreted after  $\alpha$ -secretase processing (sAPP $\alpha$ ) or AD-index calculated from Erk1/2 phosphorylation have been used as evaluation criteria for PKC modulators [17]; however, there are very few reports concerning the direct quantification of A $\beta$  in cell-based experiments. As expected, **1** enhanced APP levels in HEK293 cells overexpressing wild-type APP (HEK293-APPwt) in a dose-dependent manner (Figure 1b). By contrast, APP levels in both SH-SY5Y cells (Figure 1c) and rat primary cerebral cortex cells (Figure 1d) were largely unaltered.

### 2.2. Effects of **1** on Extracellular A $\beta$ 42/A $\beta$ 40 and A $\beta$ Oligomerization in Rat Primary Cerebral Cortex Cells

Since the amount of A $\beta$ 42 secreted by SH-SY5Y cells was near to the detection limit of specific ELISA (#27711 Human Amyloid  $\beta$  1-42 Assay Kit—IBL), we selected rat primary cerebral cortex cells for evaluating PKC modulators in the following study. After a 24 h incubation, **1** did not reduce A $\beta$ 42/A $\beta$ 40 as expected above, because the amounts of both A $\beta$ 42 and A $\beta$ 40 were lowered (Figure 2a). 12-*O*-Tetradecanoylphorbol 13-acetate (TPA) is a PKC ligand that exerts a similar effect [34]. Because the extracellular levels of toxic oligomers after a 24 h incubation were under the detection limit for specific ELISA (#27709 Human Amyloid  $\beta$  Toxic Oligomer Assay Kit—IBL) and A $\beta$ 42 easily aggregates to form amyloid fibrils after a 24 h incubation in vitro [35,36], we sampled at an earlier time point, 6 h, to determine the formation of toxic A $\beta$  oligomers. As shown in Figure 2b, the ratio of toxic oligomers to A $\beta$ 42 (toxic oligomers/A $\beta$ 42) in cerebral cortex cells did not increase following treatment with **1** even at a higher concentration range than that in Figure 2a. However, the toxic oligomer levels were unchanged by **1** (Figure 2b).

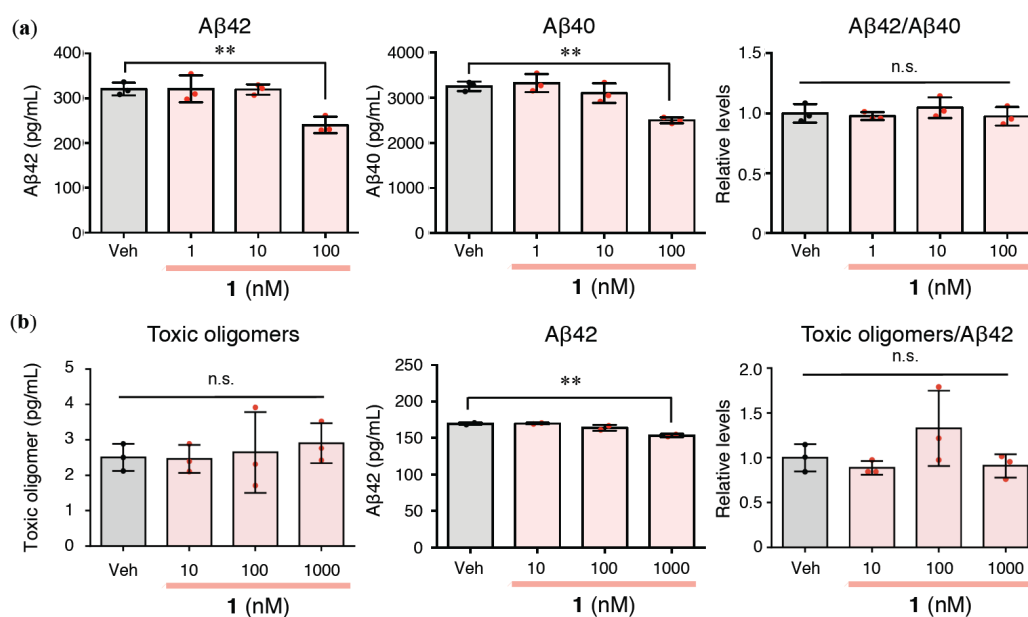


**Figure 2.** (a) Monomeric Aβ42, Aβ40, and their ratio (Aβ42/Aβ40) in the conditioned medium of rat primary cerebral cortex cells treated with **1** at the indicated concentrations for 24 h. (b) Toxic Aβ oligomers, monomeric Aβ42, and their ratio (toxic oligomers/Aβ42) in the conditioned medium of rat primary cerebral cortex cells treated with **1** at the indicated concentrations for 6 h. The data are presented as mean ± SD ( $n = 3$ ). \*\*  $p < 0.01$  versus Veh (vehicle). n.s.: not significant. Red or black dots represent each value.

### 2.3. Effects of **1** on Aβ Production and Degradation in Rat Primary Cerebral Cortex Cells

Given the moderate reduction in Aβ42 secretion to the extracellular space caused by **1** treatment (Figure 2b), we investigated the contribution of **1** to Aβ production and degradation in cultured cells. The concentration of **1** was set to 10–1000 nM in the following study of primary cultured cells. The amount of disintegrin and metalloproteinase 10 (ADAM10), as one of the α-secretases, was increased in Western blotting, using the ratio of the processed to active form of ADAM10 in the case of **1** (Figure 3a). nELAV proteins are known to act as PKCα-dependent Aβ modulators via α-secretase [12,37] or β-secretase [38]. As shown in Figure 3b, the amounts of nELAV were decreased by **1**.

Next, ECE1 levels were also measured. ECE1 levels were almost unchanged in cells treated with **1** (Figure 3c). These results indicate that the decrease in Aβ42 caused by **1** could be due to enhanced α-secretase expression, but not Aβ degradation.

### 2.4. Effects of **1** on Intracellular Aβ Oligomerization in Rat Primary Cerebral Cortex Cells

Intracellular Aβ accumulation appears to be an early event in AD pathogenesis. In particular, Aβ oligomerization may begin to induce mitochondrial toxicity, proteasome impairment, and synaptic damage [39]. To elucidate the intracellular mechanism, lysates were prepared from cells after 6 h of incubation with **1** and subjected to Western blotting using 24B3 antibody [29]. Notably, the formation of intracellular toxic oligomers, which are 20–30-mers according to synthetic studies [40,41] of Aβ oligomer models that inhibited long-term potentiation (LTP) in mouse hippocampal slices (T. Kume, personal communication, unpublished results), was significantly decreased by **1** (Figure 4). These results suggest that **1** may modulate toxic Aβ oligomerization.

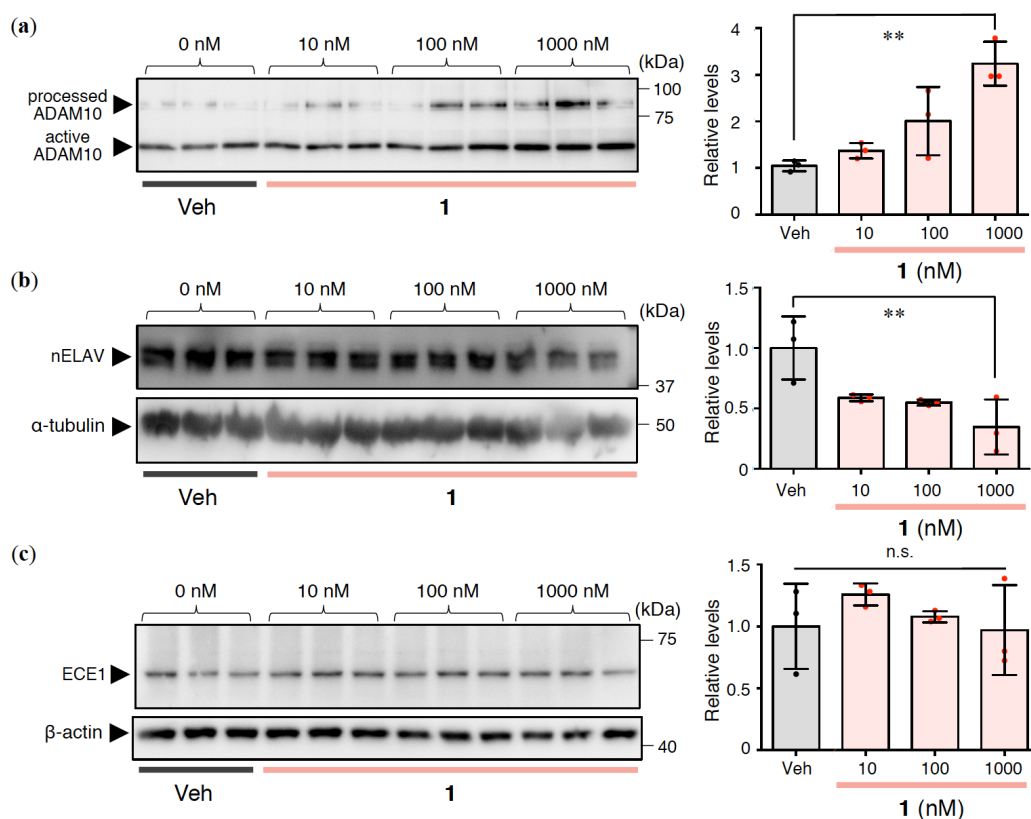


**Figure 3.** (a) Processed ADAM10, (b) nELAV, and (c) ECE1 in the cell lysate prepared from rat primary cerebral cortex cells treated with **1** at indicated concentrations for 24 h. The relative levels of (a) active ADAM10, (b)  $\alpha$ -tubulin, and (c)  $\beta$ -actin are presented as mean  $\pm$  SD ( $n = 3$ ). \*\* $p < 0.01$  versus Veh (vehicle). n.s.: not significant. Red or black dots represent each value.

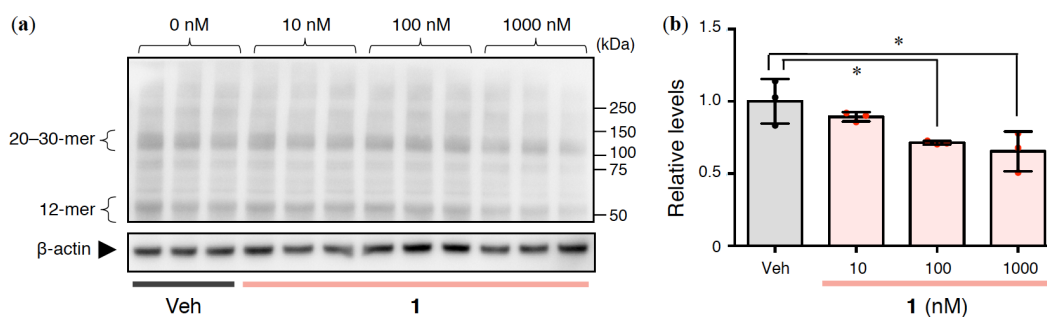


**Figure 4.** (a,b) Toxic oligomer formation in lysate from rat primary cerebral cortex cells treated with **1** at the indicated concentration for 6 h. (a) The representative Western blot shown was probed with anti-A $\beta$ 42 toxic turn (24B3) antibody. (b) Band intensities corresponding to 20–30-mers relative to  $\beta$ -actin in (a) are presented as mean  $\pm$  SD ( $n = 3$ ). \* $p < 0.05$  versus Veh (vehicle). Red or black dots represent each value.

### 2.5. Effects of **1** on the Cytotoxicity of Rat Primary Cerebral Cortex Cells

To examine the neurotoxicity of **1**, a 3-(4,5-dimethylthiazol-2-yl)-2,5-diphenyltetrazolium bromide (MTT) assay was performed on rat primary cerebral cortex cells. As shown in Figure 5, it was confirmed that **1** did not exhibit neurotoxicity at the concentrations used in the above tests (Figure 2b,3,4). This finding suggests that **1** is potentially as safe as bryo-1, with few side effects.

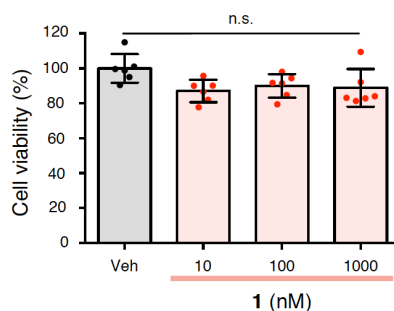


**Figure 5.** Neurotoxicity of rat primary cerebral cortex cells treated with **1** at the indicated concentrations for 24 h. The data are presented as mean  $\pm$  SD ( $n = 6$ ). n.s.: not significant. Veh: vehicle. Red or black dots represent each value.

### 2.6. Effects of **1** on A $\beta$ 42/A $\beta$ 40, A $\beta$ Oligomerization, and Neurotoxicity in Human iPS-Derived Neurons

To further verify the preventative effects of **1** against AD, human iPS-derived neurons were adopted for this experiment because of a slight difference in A $\beta$  sequence between rat and human. Recent studies also imply a large gap in the effectiveness of drug discovery studies between iPS-derived neurons and cultured cell lines [42]. Recently, Inoue and colleagues developed a reliable and robust iPS-based screening system for anti-A $\beta$  drugs [43]. After incubating the differentiated neurons from iPS with PKC ligands for 24 h, A $\beta$ 42 and A $\beta$ 40 levels in the conditioned medium were calculated using electrochemiluminescence assays. Bryo-1 was used as a positive control, which significantly decreased the amount of A $\beta$ 42 and A $\beta$ 40 in a dose-dependent manner. Bryo-1 therefore suppressed the A $\beta$ 42/A $\beta$ 40 ratio (Figure 6d). Treatment with **1** lowered A $\beta$ 42 and A $\beta$ 40 levels to almost the same extent, resulting in almost no alternation of A $\beta$ 42/A $\beta$ 40 (Figure 6a). **1** failed to show cytotoxicity such as bryo-1 (Figure 6b,e) measured by the ToxiLight assay that reflects the release of adenylate kinase from damaged cells [44].

Lysate prepared from iPS-derived neurons was subjected to ELISA measurement for toxic oligomers (Figure 6c,f). In Figure 6c, the amount of A $\beta$ 42 toxic oligomers following **1** treatment showed a tendency to decrease, like bryo-1, in a dose-dependent manner (Figure 6f), in spite of one anomalous value at 30 nM, which might originate from a technical issue. These findings suggest that **1** may also prevent toxic oligomer formation in iPS-derived neurons.

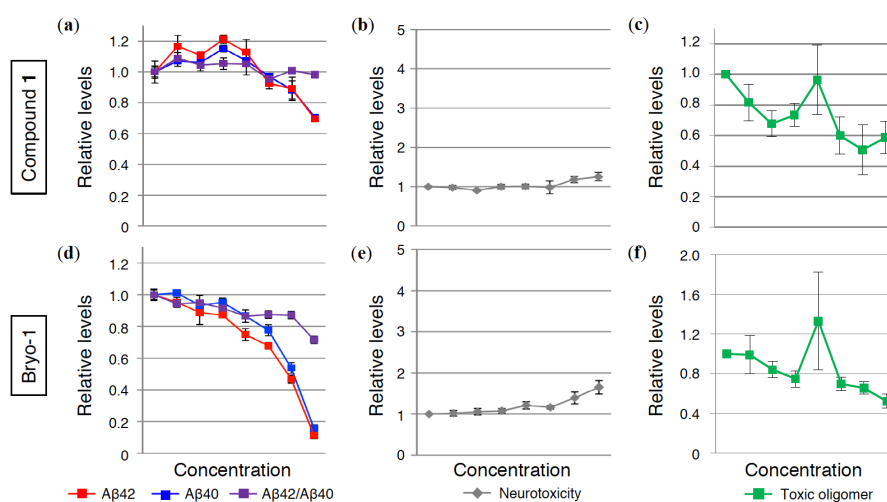


**Figure 6.** (a,d) Monomeric A $\beta$ 42, A $\beta$ 40, and A $\beta$ 42/A $\beta$ 40 in conditioned medium, (b,e) neurotoxicity, and (c,f) toxic A $\beta$ 42 oligomers in lysate from human iPS-derived neurons treated with (a,b,c) **1** and (d,e,f) bryo-1 at the indicated concentration (0, 1, 3, 10, 30, 100, 300, and 1000 nM from left to right) for 24 h. The data are presented as mean  $\pm$  SEM ( $n = 3$ ).

### 3. Discussion

Alkon and colleagues hypothesized that deficits in PKC signaling are involved in AD symptoms [18]. PKC $\alpha$  and PKC $\epsilon$  are thought to induce A $\beta$  diminution, leading to beneficial effects for AD. Indeed, the results of several clinical trials provide encouragement for bryo-1 as a potential drug against AD [45]. It is worth noting that **1** prevented nELAV accumulation within the cell (Figure 3b). nELAV levels were higher in AD patients compared with non-AD controls [38]. The nELAV-driven stabilization of  $\beta$ -secretase mRNA ( $\beta$ -site amyloid  $\beta$  precursor protein cleaving enzyme, BACE1) [38] and tau mRNA [46] may be involved in AD progression. On the other hand, experiments using SH-SY5Y cells suggest that the stabilization of ADAM10 by the binding of nELAV may contribute to beneficial effects against AD via the PKC $\alpha$  pathway [12]. Bryo-1 counteracted the deficit in ADAM10 in SH-SY5Y cells in which HuD expression had been silenced [47]. Although the involvement of nELAV in AD remains controversial, nELAV is a novel putative target for anti-AD therapies. Furthermore, Jarosz-Griffiths et al. reported that ADAM10-modulated shedding of cellular prion protein reduced the neurotoxicity of A $\beta$  oligomers [48]. The present findings illustrate that **1** prevented the formation of intracellular A $\beta$ 42 oligomers as well as extracellular A $\beta$ 42, which is associated with enhanced  $\alpha$ -secretase cleavage of APP. Further studies will be required to clarify whether **1** might affect toxic oligomerization directly, and if so, how. Given that the parent analogue (Aplog-1) of **1** can activate PKC $\delta$  [22] and **1** binds potently to the PKC $\alpha$ -C1A and PKC $\epsilon$ -C1B domains [23], **1** is a promising substitute for bryo-1 as a therapeutic drug lead for AD.

Recently, Yanagisawa and colleagues identified plasma APP669-711/A $\beta$ 42 [49] in addition to A $\beta$ 42/A $\beta$ 40 as an alternative biomarker using Japanese and Australian cohorts [50]. Using a composite biomarker calculated from APP669-711/A $\beta$ 42 and A $\beta$ 42/A $\beta$ 40 may enhance the accuracy of diagnosis during disease progression from mild cognitive impairment (MCI) to AD. However, in their work, the potential of A $\beta$  oligomerization in CSF or plasma as a biomarker was not fully addressed. Recently, a detection method for A $\beta$  oligomers using single molecule arrays (Simoa) as a highly sensitive platform was reported using the same anti-A $\beta$  N-terminal antibody (bapineuzumab), both for antigen capture and detection [51]. However, this strategy cannot exclude the possibility of detecting mature fibrils, resulting in lower specificity for A $\beta$  oligomers [52]. The use of the anti-N-terminal antibody (82E1) [53] may address the problem by using the same antibodies for capture and detection [54]. Alternatively, the development of highly specific antibodies for toxic oligomeric species with synaptotoxicity would be most ideal for finding biomarkers. In the A $\beta$ 42 toxic oligomer ELISA used in this study, the 24B3 antibody against the A $\beta$  toxic turn and 82E1 antibody against the A $\beta$  N-terminus are used for detection and capture, respectively [29].

Ohshima et al. reported that familial mutations of AD increase oligomer formation of A $\beta$  in the conditioned medium of wild-type APP-transfected cells, but intracellular levels of A $\beta$  oligomer in these mutant APP-transfected cells were unaltered compared with wild-type APP-transfected cells [55]. These results may be due to the stronger ability of A $\beta$  either to be formed or to aggregate due to these mutations in the precursor APP, namely Swedish, Dutch, and London mutations. The Osaka mutant (E693 $\Delta$ ) of A $\beta$  tends to be found as oligomers within cell bodies in both cultured cells [56] and human iPS-derived neurons [57]. It was therefore difficult to determine oligomer levels in non-mutated APP cell models with precision. Regarding the intracellular accumulation of A $\beta$ , the key question of how intracellular A $\beta$  accumulates remains unanswered, thereby invoking the involvement of tau pathology; that is, the possible interaction of intraneuronal A $\beta$  with neurofibrillary tangles [58]. The relevance of liquid–liquid phase separation to intracellular accumulation of amyloidogenic proteins (tau [59,60] and TDP-43 [61]) should also be considered.

In conclusion, to the best of our knowledge, we have developed the first direct evaluation system not only for A $\beta$  monomers, but also for their assembly into toxic oligomers in small amounts using two reliable and prevalent cell models of AD. Compared with bryo-1, whose efficiency has been recognized in several clinical trials for AD and cancer, **1** may play a pivotal role in AD prevention as a promising drug lead.

## 4. Materials and Methods

### 4.1. Rat Primary Cerebral Cortex Cells

Animals were treated according to guidelines issued by the Kyoto University Animal Experimentation Committee and by the Japanese Pharmacological Society. The experimental procedures were approved by the Kyoto University Animal Experimentation Committee [#16-12-1 (14 Mar 2016), #16-12-2 (21 Mar 2017)]. Primary cultures were obtained from the cerebral cortex of fetal Wistar rats (Nihon SLC; 17–19 d of gestation) as previously described [62]. Briefly, single cells dissociated from whole cerebral cortices of fetal rats were plated on 0.1% polyethyleneimine-coated plastic 12-well plates ( $10^6$  cells/well, 1 mL). Cells were incubated in Eagle's minimal essential medium (E-MEM) supplemented with 10% heat-inactivated fetal bovine serum (FBS) before half the medium was exchanged for fresh medium 2 and 4 d after plating. Subsequently, half the medium was exchanged for fresh medium containing 20 nM cytosine arabinoside 6 d after plating and again with fresh medium containing 10% heat-inactivated horse serum (HS) 8 d after plating. The cultures were maintained at 37 °C under a humidified 5% CO<sub>2</sub> atmosphere. Mature cerebral cortex cell cultures (10 d after plating) were used for all experiments.

DMSO stock of **1** was dissolved in E-MEM with 10% heat-inactivated HS (the concentration of DMSO in the medium was under 0.1%). After 6 or 24 h incubation, 100 µL of cell lysis buffer (RIPA buffer, Wako, Tokyo, Japan) containing a phosphatase inhibitor cocktail (Roche, Mannheim, Germany) and protease inhibitor cocktail (Roche) was added to prepare cell lysates. Supernatant was obtained by centrifugation (17,860 g, 4 °C) and stored at –80 °C until use.

### 4.2. ELISA

To determine the amounts of Aβ<sub>42</sub> [#290-62601 Human/Rat β Amyloid(42) ELISA Kit Wako (Osaka, Japan) or #27711 Human Amyloid β 1-42 Assay Kit—IBL (Gunma, Japan)] and Aβ toxic oligomers (#27709 Human Amyloid β Toxic Oligomer Assay Kit—IBL), 100 µL of cell lysate was applied to the corresponding sandwich ELISA plate.

### 4.3. Western Blotting

Total protein concentration of the brain was determined using the Bradford protein assay (Bio-Rad; Hercules, CA, USA). Brain proteins diluted to 1 µg/µL were treated with 4× LDS sample buffer (Invitrogen; Carlsbad, CA, USA) and 5 mM dithiothreitol before heating at 70 °C for 10 min. The denatured sample solution was subjected to Western blotting, following SDS-PAGE on a 10% Bis-Tris gel (Invitrogen) and subsequent transfer to PVDF (0.22 µm pore size, Bio-Rad). PVDF membranes were blocked in 2.5% ECL prime blocking (GE Healthcare; Madison, WI, USA) dissolved in phosphate-buffered saline (PBS) containing 0.5% Tween-20 (PBS-T), and incubated with primary antibody at the following dilutions: 1:1000 anti-Aβ (4G8) (Signet; Dedham, MA, USA), 1:1000 anti-APP(N) (IBL), 1:1000 anti-Aβ<sub>42</sub> toxic turn (24B3) (IBL, Gunma, Japan), 1:500 anti-ADAM10 (B-3) (IBL, Gunma, Japan), 1:140 anti-nELAV(HuD+HuC) (Santa Cruz; Santa Cruz, CA, USA), or 1:1000 anti-ECE1 (abcam; Cambridge, MA, USA). Following primary antibody incubation, blots were washed before being incubated with the appropriate secondary antibody. Blots were developed with enhanced chemiluminescence and quantified using Lumino Graph II (ATTO; Tokyo, Japan).

### 4.4. MTT Assay

Neurotoxicity was assessed by the MTT assay according to a previously reported protocol [63]. In brief, mature cerebral cortex cultures were moved to Neurobasal Medium with 2% B-27 supplement, 25 µM sodium glutamate, and penicillin/streptomycin before plating on 96-well plates ( $1.5 \times 10^6$  cells/well, 100 µL). Four days after plating, the medium was replaced with sodium glutamate-free Neurobasal Medium. Half the medium was exchanged for fresh medium 7 or 8 d after plating, and all the medium was exchanged for Neurobasal Medium with 2% B-27 supplement minus AO (Gibco; Grand Island, NY,



USA), and penicillin/streptomycin containing DMSO stock of **1** (10 d after plating). After incubation for 24 h, the culture medium was replaced with a medium containing 0.5 mg/mL MTT, and cells were incubated for 15 min at 37 °C. After removing the medium, 2-propanol (100 µL) was added to lyse the cells, and absorbance was measured at 595 nm with an absorption spectrophotometer (MultiScan JX, Thermo Scientific; Waltham, MA, USA). The absorbance measured following vehicle treatment (DMSO final concentration = 0.1%) was fixed as 100% for comparison.

#### 4.5. Generation and Characterization of Human iPS-Derived Neurons

Human iPS cells of Alzheimer's patients were generated as described from skin fibroblasts [43,57] and maintained using StemFit AK02N medium (Ajinomoto, Tokyo, Japan) [64] and expanded for neural differentiation. To establish a robust and rapid differentiation method, we utilized direct conversion technology. We differentiated iPS cells into neurons by using a direct conversion method, as previously described [43]. Briefly, we transduced human NGN2 cDNA by using the piggyBac transposon system, transiently under tetracycline-inducible promoter (tetO), and converted iPS cells into neuronal cells with more than 96% purity.

#### 4.6. Electrochemiluminescence Assays

A $\beta$  species in culture media after 24 h cultivation with PKC ligands were measured by human (6E10) A $\beta$  3-VPLex Kit (Meso Scale Discovery; Rockville, MD, USA). This assay uses the 6E10 anti- $\beta$ -amyloid antibody to capture A $\beta$  peptides and SULFO-TAG-labeled C-terminus specific anti-A $\beta$  antibodies for detection by electrochemiluminescence with Sector Imager 2400 (Meso Scale Discovery). Quantified A $\beta$  values were adjusted using total protein in neurons and compared among conditions.

#### 4.7. ToxiLight Assay

Cytotoxicity was determined to measure the release of the enzyme adenylate kinase from damaged cells [44] using The ToxiLight™ Non-destructive Cytotoxicity BioAssay Kit (Lonza; Walkersville, MD, USA). In brief, the cultured medium was collected after 24 h incubation, and applied to the assay.

#### 4.8. Statistical Analyses

The differences were subjected to one-way analysis of variance (ANOVA) followed by Bonferroni's test; *p* values < 0.05 versus vehicle were considered significant.

**Author Contributions:** Conceptualization and supervision, K.M. and K.I.; formal analysis, K.M., M.Y., S.N., and T.K. (Takayuki Kondo); investigation, K.M., M.Y., S.N., and T.K. (Takayuki Kondo); resources, T.K. (Toshiaki Kume) and H.I.; writing—original draft preparation, K.M.; writing—review and editing, K.I.; project administration, K.I. All authors have read and agreed to the published version of the manuscript.

**Acknowledgments:** We are thankful to Masahiro Maeda in IBL for providing ELISA kits. This study was in part supported by the Japanese government (Monbukagakusho: MEXT), grant number 17H06405 to K.I. and K.M. for Scientific Research on Innovative Areas 'Frontier Research on Chemical Communications', a grant for Core Center for iPS Cell Research of Research Center Network for Realization of Regenerative Medicine from AMED to H.I., and the JSPS KAKENHI, grant number 18K18452 to T.Ko. and H.I., grant number 17K16121 to T.Ko.

**Conflicts of Interest:** The authors declare no conflict of interest.

#### Abbreviations

|           |   |
|-----------|---|
| A $\beta$ | Amyloid $\beta$ -protein  |
| AD        | Alzheimer's disease   |
| ADAM10    | A disintegrin and metalloproteinase 10                            |
| APP       | Amyloid $\beta$ precursor protein                                 |
| BACE1     | $\beta$ -site amyloid $\beta$ precursor protein cleaving enzyme 1 |
| DMSO      | Dimethyl sulfoxide  |
| ECE1      | Endothelin converting enzyme 1                                    |

|       |  |
|-------|--|
| ELISA | Enzyme-linked immunosorbent assay                            |
| E-MEM | Eagle's minimal essential medium                             |
| FBS   | Fetal bovine serum   |
| HFIP  | 1,1,1,3,3,3-hexafluoro-2-propanol                            |
| HRP   | Horseradish peroxidase                                       |
| HS    | Horse serum  |
| iPS   | Induced pluripotent stem                                     |
| MCI   | Mild cognitive impairment                                    |
| MTT   | 3-(4,5-dimethylthiazol-2-yl)-2,5-diphenyltetrazolium bromide |
| PBS   | Phosphate-buffered saline                                    |
| PKC   | Protein kinase C   |
| sAPP  | Secreted amyloid $\beta$ precursor protein                   |
| WB    | Western blotting   |

## References

- Glenner, G.G.; Wong, C.W. Alzheimer's disease: initial report of the purification and characterization of a novel cerebrovascular amyloid protein. *Biochem. Biophys. Res. Commun.* **1984**, *120*, 885–890. [[CrossRef](#)]
- Masters, C.L.; Simms, G.; Weinman, N.A.; Multhaup, G.; McDonald, B.L.; Beyreuther, K. Amyloid plaque core protein in Alzheimer disease and Down syndrome. *Proc. Natl. Acad. Sci. USA* **1985**, *82*, 4245–4249. [[CrossRef](#)] [[PubMed](#)]
- Andrew, R.J.; Kellett, K.A.; Thinakaran, G.; Hooper, N.M. A Greek Tragedy: The growing complexity of Alzheimer amyloid precursor protein proteolysis. *J. Biol. Chem.* **2016**, *291*, 19235–19244. [[CrossRef](#)]
- Karran, E.; Mercken, M.; De Strooper, B. The amyloid cascade hypothesis for Alzheimer's disease: an appraisal for the development of therapeutics. *Nat. Rev. Drug Discov.* **2011**, *10*, 698–712. [[CrossRef](#)] [[PubMed](#)]
- Roychaudhuri, R.; Yang, M.; Hoshi, M.M.; Teplow, D.B. Amyloid  $\beta$ -protein assembly and Alzheimer disease. *J. Biol. Chem.* **2009**, *284*, 4749–4753. [[CrossRef](#)] [[PubMed](#)]
- Benilova, I.; Karran, E.; De Strooper, B. The toxic A $\beta$  oligomer and Alzheimer's disease: an emperor in need of clothes. *Nat. Neurosci.* **2012**, *15*, 349–357. [[CrossRef](#)] [[PubMed](#)]
- Nishizuka, Y. Protein kinase C and lipid signaling for sustained cellular responses. *FASEB J.* **1995**, *9*, 484–496. [[CrossRef](#)]
- Sun, M.K.; Alkon, D.L. The “memory kinases”: roles of PKC isoforms in signal processing and memory formation. *Prog. Mol. Biol. Transl. Sci.* **2014**, *122*, 31–59.
- Govoni, S.; Bergamaschi, S.; Racchi, M.; Battaini, F.; Binetti, G.; Bianchetti, A.; Trabucchi, M. Cytosol protein kinase C downregulation in fibroblasts from Alzheimer's disease patients. *Neurology* **1993**, *43*, 2581–2586. [[CrossRef](#)]
- Yang, H.Q.; Pan, J.; Ba, M.W.; Sun, Z.K.; Ma, G.Z.; Lu, G.Q.; Xiao, Q.; Chen, S.D. New protein kinase C activator regulates amyloid precursor protein processing in vitro by increasing  $\alpha$ -secretase activity. *Eur. J. Neurosci.* **2007**, *26*, 381–391. [[CrossRef](#)]
- Etcheberrigaray, R.; Tan, M.; Dewachter, I.; Kuiperi, C.; Van der Auwera, I.; Wera, S.; Qiao, L.; Bank, B.; Nelson, T.J.; Kozikowski, A.P.; et al. Therapeutic effects of PKC activators in Alzheimer's disease transgenic mice. *Proc. Natl. Acad. Sci. USA* **2004**, *101*, 11141–11146. [[CrossRef](#)] [[PubMed](#)]
- Pascale, A.; Amadio, M.; Scapagnini, G.; Lanni, C.; Racchi, M.; Provenzani, A.; Govoni, S.; Alkon, D.L.; Quattrone, A. Neuronal ELAV proteins enhance mRNA stability by a PKC $\alpha$ -dependent pathway. *Proc. Natl. Acad. Sci. USA* **2005**, *102*, 12065–12070. [[CrossRef](#)] [[PubMed](#)]
- Choi, D.S.; Wang, D.; Yu, G.Q.; Zhu, G.; Kharazia, V.N.; Paredes, J.P.; Chang, W.S.; Deitchman, J.K.; Mucke, L.; Messing, R.O. PKC $\epsilon$  increases endothelin converting enzyme activity and reduces amyloid plaque pathology in transgenic mice. *Proc. Natl. Acad. Sci. USA* **2006**, *103*, 8215–8220. [[CrossRef](#)] [[PubMed](#)]
- Hongpaisan, J.; Sun, M.K.; Alkon, D.L. PKC $\epsilon$  activation prevents synaptic loss, A $\beta$  elevation, and cognitive deficits in Alzheimer's disease transgenic mice. *J. Neurosci.* **2011**, *31*, 630–643. [[CrossRef](#)]
- Pacheco-Quinto, J.; Eckman, E.A. Endothelin-converting enzymes degrade intracellular  $\beta$ -amyloid produced within the endosomal/lysosomal pathway and autophagosomes. *J. Biol. Chem.* **2013**, *288*, 5606–5615. [[CrossRef](#)]

16. Pettit, G.R.; Herald, C.L.; Doubek, D.L.; Herald, D.L.; Arnold, E.; Clardy, J. Isolation and structure of bryostatin 1. *J. Am. Chem. Soc.* **1982**, *104*, 6846–6848. [[CrossRef](#)]
17. Khan, T.K.; Nelson, T.J.; Verma, V.A.; Wender, P.A.; Alkon, D.L. A cellular model of Alzheimer's disease therapeutic efficacy: PKC activation reverses A $\beta$ -induced biomarker abnormality on cultured fibroblasts. *Neurobiol. Dis.* **2009**, *34*, 332–339. [[CrossRef](#)]
18. Alkon, D.L.; Sun, M.K.; Nelson, T.J. PKC signaling deficits: a mechanistic hypothesis for the origins of Alzheimer's disease. *Trends Pharmacol. Sci.* **2007**, *28*, 51–60. [[CrossRef](#)]
19. Wender, P.A.; Hardman, C.T.; Ho, S.; Jeffreys, M.S.; Maclaren, J.K.; Quiroz, R.V.; Ryckbosch, S.M.; Shimizu, A.J.; Sloane, J.L.; Stevens, M.C. Scalable synthesis of bryostatin 1 and analogs, adjuvant leads against latent HIV. *Science* **2017**, *358*, 218–223. [[CrossRef](#)]
20. Trost, B.M.; Dong, G. Total synthesis of bryostatin 16 using atom-economical and chemoselective approaches. *Nature* **2008**, *456*, 485–488. [[CrossRef](#)]
21. Kato, Y.; Scheuer, P.J. Aplysiatoxin and debromoaplysiatoxin, constituents of the marine mollusk *Stylocheilus longicauda* (Quoy and Gaimard, 1824). *J. Am. Chem. Soc.* **1974**, *96*, 2245–2246. [[CrossRef](#)] [[PubMed](#)]
22. Nakagawa, Y.; Yanagita, R.C.; Hamada, N.; Murakami, A.; Takahashi, H.; Saito, N.; Nagai, H.; Irie, K. A simple analogue of tumor-promoting aplysiatoxin is an antineoplastic agent rather than a tumor promoter: development of a synthetically accessible protein kinase C activator with bryostatin-like activity. *Am. Chem. Soc.* **2009**, *131*, 7573–7579. [[CrossRef](#)] [[PubMed](#)]
23. Kikumori, M.; Yanagita, R.C.; Tokuda, H.; Suzuki, N.; Nagai, H.; Suenaga, K.; Irie, K. Structure-activity studies on the spiroketal moiety of a simplified analogue of debromoaplysiatoxin with antiproliferative activity. *J. Med. Chem.* **2012**, *55*, 5614–5626. [[CrossRef](#)]
24. Blennow, K.; Mattsson, N.; Scholl, M.; Hansson, O.; Zetterberg, H. Amyloid biomarkers in Alzheimer's disease. *Trends Pharmacol. Sci.* **2015**, *36*, 297–309. [[CrossRef](#)]
25. Pike, K.E.; Savage, G.; Villemagne, V.L.; Ng, S.; Moss, S.A.; Maruff, P.; Mathis, C.A.; Klunk, W.E.; Masters, C.L.; Rowe, C.C.  $\beta$ -Amyloid imaging and memory in non-demented individuals: evidence for preclinical Alzheimer's disease. *Brain* **2007**, *130*, 2837–2844. [[CrossRef](#)]
26. Rowe, C.C.; Bourgeat, P.; Ellis, K.A.; Brown, B.; Lim, Y.Y.; Mulligan, R.; Jones, G.; Maruff, P.; Woodward, M.; Price, R.; et al. Predicting Alzheimer disease with  $\beta$ -amyloid imaging: results from the Australian imaging, biomarkers, and lifestyle study of ageing. *Ann. Neurol.* **2013**, *74*, 905–913. [[CrossRef](#)]
27. Shaw, L.M.; Vanderstichele, H.; Knapik-Czajka, M.; Figurski, M.; Coart, E.; Blennow, K.; Soares, H.; Simon, A.J.; Lewczuk, P.; Dean, R.A.; et al. Qualification of the analytical and clinical performance of CSF biomarker analyses in ADNI. *Acta Neuropathol.* **2011**, *121*, 597–609. [[CrossRef](#)]
28. Irie, K. New diagnostic method for Alzheimer's disease based on the toxic conformation theory of amyloid  $\beta$ . *Biosci. Biotechnol. Biochem.* **2020**, *84*, 1–16. [[CrossRef](#)]
29. Murakami, K.; Tokuda, M.; Suzuki, T.; Irie, Y.; Hanaki, M.; Izuo, N.; Monobe, Y.; Akagi, K.; Ishii, R.; Tatebe, H.; et al. Monoclonal antibody with conformational specificity for a toxic conformer of amyloid  $\beta$ 42 and its application toward the Alzheimer's disease diagnosis. *Sci. Rep.* **2016**, *6*, 29038. [[CrossRef](#)]
30. Akiba, C.; Nakajima, M.; Miyajima, M.; Ogino, I.; Motoi, Y.; Kawamura, K.; Adachi, S.; Kondo, A.; Sugano, H.; Tokuda, T.; et al. Change of amyloid- $\beta$ 1-42 toxic conformer ratio after cerebrospinal fluid diversion predicts long-term cognitive outcome in patients with idiopathic normal pressure hydrocephalus. *J. Alzheimers Dis.* **2018**, *63*, 989–1002. [[CrossRef](#)]
31. Masuda, Y.; Uemura, S.; Ohashi, R.; Nakanishi, A.; Takegoshi, K.; Shimizu, T.; Shirasawa, T.; Irie, K. Identification of physiological and toxic conformations in A $\beta$ 42 aggregates. *ChemBioChem.* **2009**, *10*, 287–295. [[CrossRef](#)] [[PubMed](#)]
32. Trejo, J.; Massamiri, T.; Deng, T.; Dewji, N.N.; Bayney, R.M.; Brown, J.H. A direct role for protein kinase C and the transcription factor Jun/AP-1 in the regulation of the Alzheimer's  $\beta$ -amyloid precursor protein gene. *J. Biol. Chem.* **1994**, *269*, 21682–21690. [[PubMed](#)]
33. Lahiri, D.K.; Nall, C. Promoter activity of the gene encoding the  $\beta$ -amyloid precursor protein is up-regulated by growth factors, phorbol ester, retinoic acid and interleukin-1. *Brain Res. Mol. Brain Res.* **1995**, *32*, 233–240. [[CrossRef](#)]
34. Sarajarvi, T.; Jantti, M.; Paldanius, K.M.A.; Natunen, T.; Wu, J.C.; Makinen, P.; Tarvainen, I.; Tuominen, R.K.; Talman, V.; Hiltunen, M. Protein kinase C-activating isophthalate derivatives mitigate Alzheimer's disease-related cellular alterations. *Neuropharmacology* **2018**, *141*, 76–88. [[CrossRef](#)]

35. Sato, M.; Murakami, K.; Uno, M.; Nakagawa, Y.; Katayama, S.; Akagi, K.; Masuda, Y.; Takegoshi, K.; Irie, K. Site-specific inhibitory mechanism for amyloid  $\beta$ 42 aggregation by catechol-type flavonoids targeting the Lys residues. *J. Biol. Chem.* **2013**, *288*, 23212–23224. [[CrossRef](#)]
36. Yoshioka, T.; Murakami, K.; Ido, K.; Hanaki, M.; Yamaguchi, K.; Midorikawa, S.; Taniwaki, S.; Gunji, H.; Irie, K. Semisynthesis and structure-activity studies of uncarinic acid C isolated from *Uncaria rhynchophylla* as a specific inhibitor of the nucleation phase in amyloid  $\beta$ 42 aggregation. *J. Nat. Prod.* **2016**, *79*, 2521–2529. [[CrossRef](#)]
37. Amadio, M.; Pascale, A.; Wang, J.; Ho, L.; Quattrone, A.; Gandy, S.; Haroutunian, V.; Racchi, M.; Pasinetti, G.M. nELAV proteins alteration in Alzheimer's disease brain: a novel putative target for amyloid- $\beta$  reverberating on A $\beta$ PP processing. *J. Alzheimers Dis.* **2009**, *16*, 409–419. [[CrossRef](#)]
38. Kang, M.J.; Abdelmohsen, K.; Hutchison, E.R.; Mitchell, S.J.; Grammatikakis, I.; Guo, R.; Noh, J.H.; Martindale, J.L.; Yang, X.; Lee, E.K.; et al. HuD regulates coding and noncoding RNA to induce APP→A $\beta$  processing. *Cell Rep.* **2014**, *7*, 1401–1409. [[CrossRef](#)]
39. LaFerla, F.M.; Green, K.N.; Oddo, S. Intracellular amyloid- $\beta$  in Alzheimer's disease. *Nat. Rev. Neurosci.* **2007**, *8*, 499–509. [[CrossRef](#)]
40. Irie, Y.; Murakami, K.; Hanaki, M.; Hanaki, Y.; Suzuki, T.; Monobe, Y.; Takai, T.; Akagi, K.I.; Kawase, T.; Hirose, K.; et al. Synthetic models of quasi-stable amyloid  $\beta$ 40 oligomers with significant neurotoxicity. *ACS Chem. Neurosci.* **2017**, *8*, 807–816. [[CrossRef](#)]
41. Irie, Y.; Hanaki, M.; Murakami, K.; Imamoto, T.; Furuta, T.; Kawabata, T.; Kawase, T.; Hirose, K.; Monobe, Y.; Akagi, K.I.; et al. Synthesis and biochemical characterization of quasi-stable trimer models of full-length amyloid  $\beta$ 40 with a toxic conformation. *Chem. Commun.* **2018**, *55*, 182–185. [[CrossRef](#)] [[PubMed](#)]
42. Paul, S.M.; Mytelka, D.S.; Dunwiddie, C.T.; Persinger, C.C.; Munos, B.H.; Lindborg, S.R.; Schacht, A.L. How to improve R&D productivity: the pharmaceutical industry's grand challenge. *Nat. Rev. Drug Discov.* **2010**, *9*, 203–214. [[PubMed](#)]
43. Kondo, T.; Imamura, K.; Funayama, M.; Tsukita, K.; Miyake, M.; Ohta, A.; Woltjen, K.; Nakagawa, M.; Asada, T.; Arai, T.; et al. iPSC-based compound screening and in vitro trials identify a synergistic anti-amyloid  $\beta$  combination for Alzheimer's disease. *Cell Rep.* **2017**, *21*, 2304–2312. [[CrossRef](#)] [[PubMed](#)]
44. Crouch, S.P.; Kozlowski, R.; Slater, K.J.; Fletcher, J. The use of ATP bioluminescence as a measure of cell proliferation and cytotoxicity. *J. Immunol. Methods* **1993**, *160*, 81–88. [[CrossRef](#)]
45. Nelson, T.J.; Sun, M.K.; Lim, C.; Sen, A.; Khan, T.; Chirila, F.V.; Alkon, D.L. Bryostatins effects on cognitive function and PKC $\epsilon$  in Alzheimer's disease phase IIa and expanded access trials. *J. Alzheimers Dis.* **2017**, *58*, 521–535. [[CrossRef](#)]
46. Aranda-Abreu, G.E.; Behar, L.; Chung, S.; Furneaux, H.; Ginzburg, I. Embryonic lethal abnormal vision-like RNA-binding proteins regulate neurite outgrowth and tau expression in PC12 cells. *J. Neurosci.* **1999**, *19*, 6907–6917. [[CrossRef](#)]
47. Marchesi, N.; Amadio, M.; Colombrita, C.; Govoni, S.; Ratti, A.; Pascale, A. PKC activation counteracts ADAM10 deficit in HuD-silenced neuroblastoma cells. *J. Alzheimers Dis.* **2016**, *54*, 535–547. [[CrossRef](#)]
48. Jarosz-Griffiths, H.H.; Corbett, N.J.; Rowland, H.A.; Fisher, K.; Jones, A.C.; Baron, J.; Howell, G.J.; Cowley, S.A.; Chintawar, S.; Cader, M.Z.; et al. Proteolytic shedding of the prion protein via activation of metallopeptidase ADAM10 reduces cellular binding and toxicity of amyloid- $\beta$  oligomers. *J. Biol. Chem.* **2019**, *294*, 7085–7097. [[CrossRef](#)]
49. Kaneko, N.; Yamamoto, R.; Sato, T.A.; Tanaka, K. Identification and quantification of amyloid  $\beta$ -related peptides in human plasma using matrix-assisted laser desorption/ionization time-of-flight mass spectrometry. *Proc. Jpn. Acad. Ser. B. Phys. Biol. Sci.* **2014**, *90*, 104–117. [[CrossRef](#)]
50. Nakamura, A.; Kaneko, N.; Villemagne, V.L.; Kato, T.; Doecke, J.; Dore, V.; Fowler, C.; Li, Q.X.; Martins, R.; Rowe, C.; et al. High performance plasma amyloid- $\beta$  biomarkers for Alzheimer's disease. *Nature* **2018**, *554*, 249–254. [[CrossRef](#)]
51. Hwang, S.S.; Chan, H.; Sorci, M.; Van Deventer, J.; Wittrup, D.; Belfort, G.; Walt, D. Detection of amyloid  $\beta$  oligomers toward early diagnosis of Alzheimer's disease. *Anal. Biochem.* **2019**, *566*, 40–45. [[CrossRef](#)]
52. Klaver, A.C.; Patrias, L.M.; Finke, J.M.; Loeffler, D.A. Specificity and sensitivity of the A $\beta$  oligomer ELISA. *J. Neurosci. Methods* **2011**, *195*, 249–254. [[CrossRef](#)]

53. Horikoshi, Y.; Mori, T.; Maeda, M.; Kinoshita, N.; Sato, K.; Yamaguchi, H. A $\beta$  N-terminal-end specific antibody reduced  $\beta$ -amyloid in Alzheimer-model mice. *Biochem. Biophys. Res. Commun.* **2004**, *325*, 384–387. [[CrossRef](#)]
54. Xia, W.; Yang, T.; Shankar, G.; Smith, I.M.; Shen, Y.; Walsh, D.M.; Selkoe, D.J. A specific enzyme-linked immunosorbent assay for measuring  $\beta$ -amyloid protein oligomers in human plasma and brain tissue of patients with Alzheimer disease. *Arch. Neurol.* **2009**, *66*, 190–199. [[CrossRef](#)]
55. Ohshima, Y.; Taguchi, K.; Mizuta, I.; Tanaka, M.; Tomiyama, T.; Kametani, F.; Yabe-Nishimura, C.; Mizuno, T.; Tokuda, T. Mutations in the  $\beta$ -amyloid precursor protein in familial Alzheimer's disease increase A $\beta$  oligomer production in cellular models. *Heliyon* **2018**, *4*, e00511. [[CrossRef](#)]
56. Umeda, T.; Ramser, E.M.; Yamashita, M.; Nakajima, K.; Mori, H.; Silverman, M.A.; Tomiyama, T. Intracellular amyloid  $\beta$  oligomers impair organelle transport and induce dendritic spine loss in primary neurons. *Acta Neuropathol. Commun.* **2015**, *3*, 51. [[CrossRef](#)]
57. Kondo, T.; Asai, M.; Tsukita, K.; Kutoku, Y.; Ohsawa, Y.; Sunada, Y.; Imamura, K.; Egawa, N.; Yahata, N.; Okita, K.; et al. Modeling Alzheimer's disease with iPSCs reveals stress phenotypes associated with intracellular A $\beta$  and differential drug responsiveness. *Cell Stem Cell* **2013**, *12*, 487–496. [[CrossRef](#)]
58. Guo, J.P.; Arai, T.; Miklossy, J.; McGeer, P.L. A $\beta$  and tau form soluble complexes that may promote self aggregation of both into the insoluble forms observed in Alzheimer's disease. *Proc. Natl. Acad. Sci. USA* **2006**, *103*, 1953–1958. [[CrossRef](#)]
59. Ambadipudi, S.; Biernat, J.; Riedel, D.; Mandelkow, E.; Zweckstetter, M. Liquid-liquid phase separation of the microtubule-binding repeats of the Alzheimer-related protein Tau. *Nat. Commun.* **2017**, *8*, 275. [[CrossRef](#)]
60. Boyko, S.; Qi, X.; Chen, T.H.; Surewicz, K.; Surewicz, W.K. Liquid-liquid phase separation of tau protein: The crucial role of electrostatic interactions. *J. Biol. Chem.* **2019**, *294*, 11054–11059. [[CrossRef](#)]
61. Vogler, T.O.; Wheeler, J.R.; Nguyen, E.D.; Hughes, M.P.; Britson, K.A.; Lester, E.; Rao, B.; Betta, N.D.; Whitney, O.N.; Ewachiw, T.E.; et al. TDP-43 and RNA form amyloid-like myo-granules in regenerating muscle. *Nature* **2018**, *563*, 508–513. [[CrossRef](#)]
62. Kume, T.; Kouchiyama, H.; Kaneko, S.; Maeda, T.; Akaike, A.; Shimohama, S.; Kihara, T.; Kimura, J.; Wada, K.; Koizumi, S. BDNF prevents NO mediated glutamate cytotoxicity in cultured cortical neurons. *Brain Res* **1997**, *756*, 200–204. [[CrossRef](#)]
63. Izuo, N.; Kume, T.; Sato, M.; Murakami, K.; Irie, K.; Izumi, Y.; Akaike, A. Toxicity in rat primary neurons through the cellular oxidative stress induced by the turn formation at positions 22 and 23 of A $\beta$ 42. *ACS Chem. Neurosci.* **2012**, *3*, 674–681. [[CrossRef](#)]
64. Nakagawa, M.; Taniguchi, Y.; Senda, S.; Takizawa, N.; Ichisaka, T.; Asano, K.; Morizane, A.; Doi, D.; Takahashi, J.; Nishizawa, M.; et al. A novel efficient feeder-free culture system for the derivation of human induced pluripotent stem cells. *Sci. Rep.* **2014**, *4*, 3594. [[CrossRef](#)]

